

Up-down Asymmetries and Angular Distributions in $D \rightarrow K_1(\rightarrow K\pi\pi)\ell^+\nu_\ell$

Lingzhu Bian¹, Liang Sun¹, Wei Wang²

¹ School of Physics and Technology, Wuhan University, Wuhan, China

² INPAC, Key Laboratory for Particle Astrophysics and Cosmology (MOE),
Shanghai Key Laboratory for Particle Physics and Cosmology,

School of Physics and Astronomy, Shanghai Jiao Tong University, Shanghai 200240, China

Using the helicity amplitude technique, we derive differential decay widths and angular distributions for the decay cascade $D \rightarrow K_1(1270, 1400)\ell^+\nu_\ell \rightarrow (K\pi\pi)\ell^+\nu_\ell$ ($\ell = e, \mu$), in which the electron and muon mass is explicitly included. Using a set of phenomenological results for $D \rightarrow K_1$ form factors, we calculate partial decay widths and branching fractions for $D^0 \rightarrow K_1^-\ell^+\nu_\ell$ and $D^+ \rightarrow K_1^0\ell^+\nu_\ell$, but find that results for $\mathcal{B}(D \rightarrow K_1(1270)e^+\nu_e)$ are larger than recent BESIII measurements by about a factor 1.5. We further demonstrate that the measurement of up-down asymmetry in $D \rightarrow K_1e^+\nu_e \rightarrow (K\pi\pi)e^+\nu_e$ and angular distributions in $D \rightarrow K_1\ell^+\nu_\ell \rightarrow (K\pi\pi)\ell^+\nu_\ell$ can help to determine the hadronic amplitude requested in $B \rightarrow K_1(\rightarrow K\pi\pi)\gamma$. Based on the Monte-Carlo simulation with the LHCb geometrical acceptance, we find that the angular distributions of MC events can be well described.

I. INTRODUCTION

Since the establishment of standard model (SM) in 1960s, searching for new physics (NP) beyond SM has become a most primary objective in particle physics. This can in principle proceed in two distinct directions. It is likely that new particles emerge directly in high energy collisions for instance at large hadron collider (LHC). On the other side, NP particles can affect various low-energy observables by modifying the coupling strength or introducing new interaction forms and thus a high precision study of these observables is likely to indirectly access the NP. In the SM, the charged weak interaction has the $V - A$ chirality and thereby the photon in $b \rightarrow s\gamma$ is predominantly left-handed. The contribution with right-handed polarization is suppressed by the ratio of strange and bottom quark masses. Therefore the measurement of photon polarization in $b \rightarrow s\gamma$ provides a unique probe for new physics [1–3]. A representative scenario of this type is the left-right symmetric model [4, 5], in which the photon can acquire a significant right-handed component.

In practice, the chirality of the $b \rightarrow s\gamma$ can be detected using the measurements of inclusive $B \rightarrow X_s\gamma$ decay branching fractions [6–9], the mixing-induced CP asymmetries of radiative B^0 and B_s^0 decays [10–13] and the $B \rightarrow K^*e^+e^-$ with very low dilepton mass squared [14, 15]. Interestingly, the photon helicity in radiative D decays was also explored [16].

In addition to the above methods, it is pointed out that the photon helicity in $b \rightarrow s\gamma$ is proportional to an up-down asymmetry \mathcal{A}_{UD} in $B \rightarrow K_1(\rightarrow K\pi\pi)\gamma$ [17–19] and more generally the angular distribution in $B \rightarrow K_{res}(\rightarrow K\pi\pi)\gamma$. Throughout this work we will use K_1 to abbreviate the axial-vector meson $K_1(1270)$ and/or $K_1(1400)$. However the measurement of up-down asymmetry in $B \rightarrow K_1\gamma$ [20] alone was incapable to reveal the photon helicity due to the entanglement with the K_1 decay dynamics. Many interesting theoretical analyses have adopted nonperturbative approaches to parametrize the $K_1 \rightarrow K\pi\pi$ decay amplitude and power constraints on the decay parameters were obtained [17–19, 21, 22]. In a previous work [23] it is proposed that one can tackle this problem by combining semileptonic $D \rightarrow K_1e^+\nu_e$ decays. In particular, a ratio of up-down asymmetries in $D \rightarrow K_1(\rightarrow K\pi\pi)e^+\nu_e$, \mathcal{A}'_{UD} , has been proposed to quantify the hadronic effects in $K_1 \rightarrow K\pi\pi$ decay. More explicitly the photon helicity can be expressed as a ratio of the two observables $\lambda_\gamma = 3/4 \times \mathcal{A}_{UD}/\mathcal{A}'_{UD}$ [23].

The purpose of this work is multifold. We will first give the details in the helicity amplitude approach to derive the pertinent angular distributions and up-down asymmetries. Secondly we will extend the previous analysis to the muon mode whose mass can not be neglected in D decays. Using the phenomenological results for $D \rightarrow K_1$ form factors, we calculate partial decay widths for $D \rightarrow K_1\ell^+\nu_\ell$, and show that the measurement of up-down asymmetry in $D \rightarrow K_1(\rightarrow K\pi\pi)e^+\nu_e$ and the angular distribution in $D \rightarrow K_1(\rightarrow K\pi\pi)\ell^+\nu_\ell$ can help to determine the hadronic amplitude requested in $B \rightarrow K_1(\rightarrow K\pi\pi)\gamma$. Based on the Monte Carlo (MC) simulation with the LHCb geometrical acceptance, we find that the angular distributions of MC events can be well described.

The rest of this paper is organized as follows. In Sec. II, we will give a detailed derivation of the angular distributions. In Sec. III, we will use the $D \rightarrow K_1$ form factors and calculate the differential decay widths. A comparison of predicted branching fractions with BESIII measurements is made, and a MC simulation of angular distributions with the LHCb geometrical acceptance is also presented. The last section contains a brief summary.

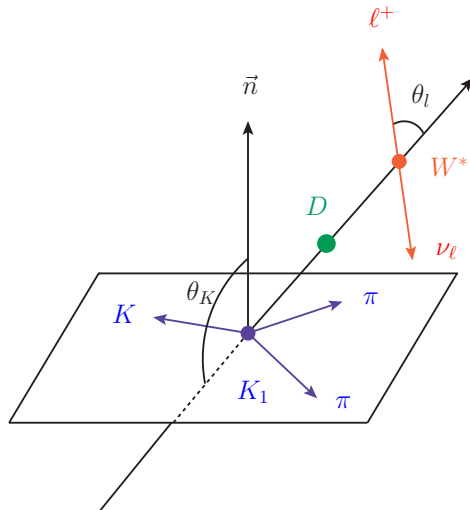


FIG. 1: The kinematics for $D \rightarrow K_1 \ell^+ \nu_\ell \rightarrow (K\pi\pi)\ell^+ \nu_\ell$. In the lepton pair $\ell^+ \nu_\ell$ rest frame, the angle θ_ℓ is defined by the ℓ^+ flight direction and the opposite of the D meson flight direction. In the K_1 rest frame the \vec{n} is defined as the normal direction of the K_1 decay plane, and θ_K is the relative angle between \vec{n} and the opposite of the D flight direction. Under parity transformation, the D flight direction will be reversed, but since \vec{n} is a cross product of two momenta, its direction is unchanged. Accordingly the θ_K will be changed to $\pi - \theta_K$ under parity transformation, implying that the $\cos \theta_K$ is parity odd.

II. FRAMEWORK AND ANGULAR DISTRIBUTIONS

In this section we will make use of the helicity amplitude technique and derive the angular distributions for the decay cascade $D \rightarrow K_1 \ell^+ \nu_\ell \rightarrow (K\pi\pi)\ell^+ \nu_\ell$. Here the D and K_1 could be charged or neutral. Since a neutral π^0 is difficult to reconstruct especially at hadron colliders, it is more plausible to explore the $\pi^+\pi^-$ final state. Thus we will mainly consider the decay chain $D^0 \rightarrow K_1^- \ell^+ \nu_\ell \rightarrow (K^- \pi^+ \pi^-)\ell^+ \nu_\ell$ and $D^+ \rightarrow \bar{K}_1^0 \ell^+ \nu_\ell \rightarrow (\bar{K}^0 \pi^+ \pi^-)\ell^+ \nu_\ell$, though the results are also applicable to other decay channels with neutral pions. The kinematics of this decay cascade is shown in Fig. 1. In the lepton pair $\ell^+ \nu_\ell$ rest frame, θ_ℓ is defined by the ℓ^+ flight direction and the opposite of the D meson flight direction. In K_1 rest frame, \vec{n} is defined as the normal direction of the decay plane, and θ_K is the relative angle between \vec{n} and the opposite of the D meson flight direction.

A few remarks on the kinematics are given in order.

- The normal direction is not unambiguous. For instance, in K_1^- decay plane, it is likely to construct the normal direction with the momentum of π^+ and π^- , while the LHCb measurement of up-down asymmetry and angular distributions in $B \rightarrow K_1 \gamma$ makes use of the slow and fast pion momentum [20], $\vec{n} \sim \vec{p}_{\pi, \text{slow}} \times \vec{p}_{\pi, \text{fast}}$.
- Secondly, under parity transformation, the D flight direction will be reversed, but since \vec{n} is a cross product of two momenta, its direction is unchanged. Accordingly the θ_K will be changed to $\pi - \theta_K$ under parity transformation, implying that the $\cos \theta_K$ is parity odd. The left-handed and right-handed polarization of K_1 gives opposite contributions to the $\cos \theta_K$ term.
- Thirdly, weak interaction in $W^* \rightarrow \ell^+ \nu_\ell$ violates parity conservation. Thus even though $\cos \theta_\ell$ is parity-even, the left-handed and right-handed contributions to the $\cos \theta_\ell$ term also differ in sign.
- Furthermore the definition of θ_K depends on charge or flavor of K_1 , namely the angle θ_K defined in K_1^- decay may differ with the one defined in K_1^+ system. It is important to stick with the same convention on the kinematics in analyzing B and D decays.

Semileptonic decays of D into K_1 are induced by effective electro-weak Hamiltonian:

$$\mathcal{H} = \frac{G_F}{\sqrt{2}} V_{cs} \bar{s} \gamma^\mu (1 - \gamma_5) c \times \bar{\nu}_\ell \gamma_\mu (1 - \gamma_5) \ell, \quad (1)$$

where G_F is Fermi constant, and V_{cs} is CKM matrix element. With the above Hamiltonian, the partial decay width

for semileptonic D decays can be generically written as

$$d\Gamma = \frac{(2\pi)^4}{2m_D} \times d\Phi_n \times \sum_{spin} |\mathcal{M}|^2. \quad (2)$$

Here $d\Phi_n$ denotes the n -body phase space. The pertinent decay amplitude \mathcal{M} can be decomposed into three individuals: $D \rightarrow K_1 W^*$, $K_1 \rightarrow K\pi\pi$ and $W^* \rightarrow \ell^+ \nu_\ell$. Using the relation between $g_{\mu\nu}$ and polarization vector,

$$g_{\mu\nu} = - \sum_{\lambda=0,\pm 1} \epsilon_\mu^*(\lambda) \epsilon_\nu(\lambda) + \frac{q_\mu q_\nu}{q^2}, \quad (3)$$

one can disassemble decay amplitudes into a hadronic part and leptonic part

$$\begin{aligned} \mathcal{M} &= \frac{G_F}{\sqrt{2}} V_{cs} H^\mu L^\nu g_{\mu\nu} \\ &= \frac{G_F}{\sqrt{2}} V_{cs} \left[- \sum_\lambda H \cdot \epsilon^*(\lambda) \times L \cdot \epsilon(\lambda) + H \cdot \epsilon^*(t) \times L \cdot \epsilon(t) \right], \end{aligned} \quad (4)$$

with $\epsilon^\mu(t) \equiv q^\mu / \sqrt{q^2}$. After the decomposition, both hadronic and leptonic parts are Lorentz invariant and thus can be calculated in convenient reference frames. Actually the hadronic part could be further resolved into two individuals, namely $D \rightarrow K_1 W^*$ and $K_1 \rightarrow K\pi\pi$. Each individuals will be calculated in rest frame of the decaying parent particle.

A. The leptonic amplitude for $W^* \rightarrow \ell^+ \nu_\ell$

For simplicity, we introduce the abbreviation,

$$\begin{aligned} L(\lambda_e, \lambda_\nu, \lambda_W = 0, \pm 1) &= L^\mu \epsilon_\mu(\lambda) = \bar{u}_\nu \gamma^\mu (1 - \gamma_5) v_\ell \epsilon_\mu(\lambda), \\ L(\lambda_e, \lambda_\nu, \lambda_W = t) &= L^\mu \frac{q_\mu}{\sqrt{q^2}} = \bar{u}_\nu \gamma^\mu (1 - \gamma_5) v_\ell \frac{q_\mu}{\sqrt{q^2}}, \end{aligned} \quad (5)$$

where all spin/helicity indices are explicitly shown. Introducing $f_l = i\sqrt{2(q^2 - m_\ell^2)}$ and using $\hat{m}_\ell = m_\ell / \sqrt{q^2}$, one can obtain the non-vanishing leptonic decay amplitude:

$$\begin{aligned} L\left(\lambda_e = -\frac{1}{2}, \lambda_\nu = -\frac{1}{2}, \lambda_W = -1\right) &= f_l \hat{m}_\ell \sin \theta_\ell, & L\left(\lambda_e = -\frac{1}{2}, \lambda_\nu = -\frac{1}{2}, \lambda_W = 0\right) &= -f_l \sqrt{2} \hat{m}_\ell \cos \theta_\ell, \\ L\left(\lambda_e = -\frac{1}{2}, \lambda_\nu = -\frac{1}{2}, \lambda_W = 1\right) &= -f_l \hat{m}_\ell \sin \theta_\ell, & L\left(\lambda_e = -\frac{1}{2}, \lambda_\nu = -\frac{1}{2}, t\right) &= f_l \sqrt{2} \hat{m}_\ell \\ L\left(\lambda_e = \frac{1}{2}, \lambda_\nu = -\frac{1}{2}, \lambda_W = -1\right) &= -f_l (1 + \cos \theta_\ell), & L\left(\lambda_e = \frac{1}{2}, \lambda_\nu = -\frac{1}{2}, \lambda_W = 0\right) &= -f_l \sqrt{2} \sin \theta_\ell, \\ L\left(\lambda_e = \frac{1}{2}, \lambda_\nu = -\frac{1}{2}, \lambda_W = 1\right) &= -f_l (1 - \cos \theta_\ell). \end{aligned} \quad (6)$$

In the massless limit $m_\ell \rightarrow 0$, only the last three terms are non-zero due to the helicity conservation.

B. $D \rightarrow K_1 W^*$

The $D \rightarrow K_1$ transition matrix element is parameterized by a set of form factors:

$$\langle K_1 | \bar{s} \gamma^\mu \gamma_5 c | D \rangle = - \frac{2iA(q^2)}{m_D - m_{K_1}} \epsilon^{\mu\nu\rho\sigma} (\epsilon_{K_1}^*)_\nu (p_D)_\rho (p_{K_1})_\sigma, \quad (7)$$

$$\begin{aligned} \langle K_1 | \bar{s} \gamma^\mu c | D \rangle &= -2m_{K_1} V_0(q^2) \frac{\epsilon_{K_1}^* \cdot q}{q^2} q^\mu - (m_D - m_{K_1}) V_1(q^2) [\epsilon_{K_1}^* - \frac{\epsilon_{K_1}^* \cdot q}{q^2} q^\mu] \\ &\quad + V_2(q^2) \frac{\epsilon_{K_1}^* \cdot q}{m_D - m_{K_1}} [(p_D + p_{K_1})^\mu - \frac{m_D^2 - m_{K_1}^2}{q^2} q^\mu], \end{aligned} \quad (8)$$

where $q^\mu = p_D^\mu - p_{K_1}^\mu$ is the momentum transfer and $\epsilon^{\mu\nu\rho\sigma}$ is the anti-symmetric Levi-Civita tensor. So the matrix element $c_{\lambda_W} \equiv \langle K_1 | \bar{s} \gamma^\mu (1 - \gamma_5) c | D \rangle \epsilon_\mu^*(\lambda_W)$ is evaluated as

$$c_\pm = (m_D - m_{K_1})V_1 \mp \frac{A\sqrt{\lambda(m_D^2, m_{K_1}^2, q^2)}}{m_D - m_{K_1}}, \quad (9)$$

$$c_0 = \frac{-1}{2m_{K_1}\sqrt{q^2}} \left[(m_D^2 - m_{K_1}^2 - q^2)(m_D - m_{K_1})V_1 - \frac{\lambda(m_D^2, m_{K_1}^2, q^2)}{m_D - m_{K_1}}V_2 \right], \quad (10)$$

$$c_t = -\frac{\sqrt{\lambda(m_D^2, m_{K_1}^2, q^2)}}{\sqrt{q^2}}V_0. \quad (11)$$

In the above, $\lambda(m_D^2, m_{K_1}^2, q^2) = (m_D^2 + m_{K_1}^2 - q^2)^2 - 4m_D^2m_{K_1}^2$.

C. Differential decay width for $D \rightarrow K_1\ell^+\nu_\ell$

In this subsection, we will derive the differential decay width for $D \rightarrow K_1\ell^+\nu_\ell$, which serves as a normalization for the angular distributions for $D \rightarrow K_1(\rightarrow K\pi\pi)\ell^+\nu_\ell$ in the narrow width limit $\Gamma_{K_1} \rightarrow 0$.

Combining the three-body phase space

$$\begin{aligned} d\Phi_3(p_{K_1}, p_\ell, p_{\nu_\ell}) &= \delta^4(p_D - p_{K_1} - p_\ell - p_{\nu_\ell}) \frac{d^3p_{K_1}}{(2\pi)^3 2E_{K_1}} \frac{d^3p_{\ell^+}}{(2\pi)^3 2E_{\ell^+}} \frac{d^3p_{\nu_\ell}}{(2\pi)^3 2E_{\nu_\ell}} \\ &= \delta^4(p_D - p_{K_1} - q)(2\pi)^4 \delta^4(q - p_{\ell^+} - p_{\nu_\ell}) \frac{d^4q}{(2\pi)^4} \frac{d^3p_{K_1}}{(2\pi)^3 2E_{K_1}} \frac{d^3p_{\ell^+}}{(2\pi)^3 2E_{\ell^+}} \frac{d^3p_{\nu_\ell}}{(2\pi)^3 2E_{\nu_\ell}} \\ &= \frac{1}{(2\pi)^7} \frac{\sqrt{\lambda(m_D^2, m_{K_1}^2, q^2)}}{32m_D^2} (1 - m_\ell^2/q^2) \times d\cos\theta_\ell dq^2, \end{aligned} \quad (12)$$

one can obtain the angular distribution for $D \rightarrow K_1\ell^+\nu_\ell$

$$\begin{aligned} \frac{d\Gamma}{dq^2 d\cos\theta_\ell} &= \frac{G_F^2 |V_{cs}|^2 \sqrt{\lambda(m_D^2, m_{K_1}^2, q^2)} q^2}{512\pi^3 m_D^3} (1 - \hat{m}_\ell^2)^2 \times \left(2c_0^2 (\sin^2\theta_\ell + \hat{m}_\ell^2 \cos^2\theta_\ell) \right. \\ &\quad \left. + c_+^2 [(1 + \cos\theta_\ell)^2 + \hat{m}_\ell^2 \sin^2\theta_\ell] + c_-^2 [(1 - \cos\theta_\ell)^2 + \hat{m}_\ell^2 \sin^2\theta_\ell] + c_t^2 2\hat{m}_t^2 - \text{Re}[c_0 c_t^*] 4\hat{m}_t^2 \cos\theta \right). \end{aligned} \quad (13)$$

Integrating over $\cos\theta_\ell$, one can have partial decay widths [24, 25]:

$$\begin{aligned} \frac{d\Gamma_L(D \rightarrow K_1\ell^+\nu_\ell)}{dq^2} &= \frac{G_F^2 |V_{cs}|^2 \sqrt{\lambda(m_D^2, m_{K_1}^2, q^2)} q^2}{512\pi^3 m_D^3} (1 - \hat{m}_\ell^2)^2 \times \left(\frac{4}{3} c_0^2 (2 + \hat{m}_\ell^2) + 4\hat{m}_\ell^2 c_t^2 \right) \\ &= \frac{\sqrt{\lambda(m_D^2, m_{K_1}^2, q^2)} G_F^2 |V_{cs}|^2}{384m_D^3 \pi^3} (1 - \hat{m}_\ell^2)^2 \times \left\{ 3\hat{m}_t^2 \lambda(m_D^2, m_{K_1}^2, q^2) V_0^2 \right. \\ &\quad \left. + (\hat{m}_\ell^2 + 2) \left| \frac{1}{2m_{K_1}} [(m_D^2 - m_{K_1}^2 - q^2)(m_D - m_{K_1})V_1 - \frac{\lambda(m_D^2, m_{K_1}^2, q^2)}{m_D - m_{K_1}}V_2] \right|^2 \right\}, \end{aligned} \quad (14)$$

$$\begin{aligned} \frac{d\Gamma_\pm(D \rightarrow K_1\ell^+\nu_\ell)}{dq^2} &= \frac{G_F^2 |V_{cs}|^2 \sqrt{\lambda(m_D^2, m_{K_1}^2, q^2)} q^2}{512\pi^3 m_D^3} (1 - \hat{m}_\ell^2)^2 \times \frac{4}{3} c_\pm^2 (2 + \hat{m}_\ell^2) \\ &= \frac{\sqrt{\lambda(m_D^2, m_{K_1}^2, q^2)} G_F^2 |V_{cs}|^2}{384m_D^3 \pi^3} (1 - \hat{m}_\ell^2)^2 q^2 \\ &\quad \times \left\{ (\hat{m}_\ell^2 + 2) \lambda(m_D^2, m_{K_1}^2, q^2) \left| \frac{A}{m_D - m_{K_1}} \mp \frac{(m_D - m_{K_1})V_1}{\sqrt{\lambda(m_D^2, m_{K_1}^2, q^2)}} \right|^2 \right\}, \end{aligned} \quad (15)$$

where L and \pm in the subscripts denote contribution from longitudinal and transverse polarization.

D. $K_1 \rightarrow K\pi\pi$

The hadronic part in the decay cascade $D \rightarrow K_1\ell^+\nu_\ell \rightarrow (K\pi\pi)\ell^+\nu_\ell$ contains:

$$H \cdot \epsilon_W^*(\lambda) \sim \langle K\pi\pi|K_1 \rangle \times \langle K_1|(V-A)_\mu|D \rangle \epsilon_W^{*\mu}(\lambda), \quad (16)$$

where $\langle K\pi\pi|K_1 \rangle$ is parameterized as

$$\langle K\pi\pi|K_1 \rangle = (2\pi)^4 \delta^4(p_{K_1} - p_K - p_\pi - p_\pi) \times \epsilon_{K_1} \cdot J. \quad (17)$$

Notice that the explicit form of J depends on the convention of the \vec{n} .

In the K_1 rest frame, one can set the normal direction as the z -axis and the momenta of (K, π^+, π^-) lies in the $x-y$ plane. Since J is a linear combination of the momenta of two pions, $J_z = 0$ and

$$J_\mu = (J_0, J_x, J_y, 0). \quad (18)$$

To simplify the calculation, we choose K_1 moving along (θ_K, ϕ) direction, and thus $\epsilon_{K_1} \cdot J$ is evaluated as

$$\epsilon_{K_1}(0) \cdot J = \sin\theta_K(J_x \cos\phi + J_y \sin\phi), \quad (19)$$

$$\epsilon_{K_1}(1) \cdot J = -\frac{1}{\sqrt{2}}[\cos\phi(J_x \cos\theta_K + iJ_y) + \sin\phi(J_y \cos\theta_K - iJ_x)], \quad (20)$$

$$\epsilon_{K_1}(-1) \cdot J = \frac{1}{\sqrt{2}}[\cos\phi(J_x \cos\theta_K - iJ_y) + \sin\phi(J_y \cos\theta_K + iJ_x)]. \quad (21)$$

E. Angular Distributions in $D \rightarrow K_1\ell^+\nu_\ell \rightarrow (K\pi\pi)\ell^+\nu_\ell$

With the above individuals, one obtains the total decay amplitude:

$$\begin{aligned} \mathcal{M}(\lambda_\ell = -\frac{1}{2}) &= L \left(\lambda_e = -\frac{1}{2}, \lambda_\nu = -\frac{1}{2}, \lambda_W = -1 \right) \times \epsilon_{K_1}(-1) \cdot J \times c_- \\ &\quad + L \left(\lambda_\ell = -\frac{1}{2}, \lambda_\nu = -\frac{1}{2}, \lambda_W = 1 \right) \times \epsilon_{K_1}(1) \cdot J \times c_+ \\ &\quad + L \left(\lambda_\ell = -\frac{1}{2}, \lambda_\nu = -\frac{1}{2}, \lambda_W = 0 \right) \times \epsilon_{K_1}(0) \cdot J \times c_0 \\ &\quad - L \left(\lambda_\ell = -\frac{1}{2}, \lambda_\nu = -\frac{1}{2}, \lambda_W = t \right) \times \epsilon_{K_1}(0) \cdot J \times c_t, \end{aligned} \quad (22)$$

$$\begin{aligned} \mathcal{M}(\lambda_\ell = \frac{1}{2}) &= L \left(\lambda_e = \frac{1}{2}, \lambda_\nu = -\frac{1}{2}, \lambda_W = -1 \right) \times \epsilon_{K_1}(-1) \cdot J \times c_- \\ &\quad + L \left(\lambda_\ell = \frac{1}{2}, \lambda_\nu = -\frac{1}{2}, \lambda_W = 1 \right) \times \epsilon_{K_1}(1) \cdot J \times c_+ \\ &\quad + L \left(\lambda_\ell = \frac{1}{2}, \lambda_\nu = -\frac{1}{2}, \lambda_W = 0 \right) \times \epsilon_{K_1}(0) \cdot J \times c_0 \\ &\quad - L \left(\lambda_e = \frac{1}{2}, \lambda_\nu = -\frac{1}{2}, \lambda_W = t \right) \times \epsilon_{K_1}(0) \cdot J \times c_t. \end{aligned} \quad (23)$$

Using two abbreviations:

$$|J|^2 = |J_x|^2 + |J_y|^2, \quad \text{Im}[n \cdot (\vec{J} \times \vec{J}^*)] = -i(J_x J_y^* - J_y J_x^*), \quad (24)$$

and integrating over ϕ , we obtain:

$$\begin{aligned} |\mathcal{M}|^2 &= \frac{3}{4\pi|J|^2} \int d\phi (|\mathcal{M}(\lambda_e = \frac{1}{2})|^2 + |\mathcal{M}(\lambda_e = -\frac{1}{2})|^2) \\ &= \frac{3}{8} (d_1 + d'_1 [\cos^2\theta_K \cos^2\theta_\ell] + d_2 \cos\theta_\ell + d'_2 \cos^2\theta_K \cos\theta_\ell \\ &\quad + d_3 \cos\theta_K + d'_3 \cos\theta_K \cos^2\theta_\ell + d_4 \cos\theta_K \cos\theta_\ell + d_5 \cos^2\theta_K + d'_5 \cos^2\theta_\ell), \end{aligned} \quad (25)$$

where a factor $\frac{3}{4\pi|J|^2}$ is introduced to be consistent with the three-body decay width. In the above equation, the angular coefficients are calculated as

$$\begin{aligned}
d_1 &= (1 + \hat{m}_\ell^2)(|c_-|^2 + |c_+|^2) + 4|c_0|^2 + 4\hat{m}_\ell^2|c_t|^2, \\
d'_1 &= (1 - \hat{m}_\ell^2)(4|c_0|^2 + |c_-|^2 + |c_+|^2), \\
d_2 &= -2[|c_-|^2 - |c_+|^2 + 4\text{Re}[c_0c_t^*]\hat{m}_\ell^2], \\
d'_2 &= -2[|c_-|^2 - |c_+|^2 - 4\text{Re}[c_0c_t^*]\hat{m}_\ell^2], \\
d_3 &= 2\frac{\text{Im}[\vec{n} \cdot (\vec{J} \times \vec{J}^*)]}{|J|^2}[(1 + \hat{m}_\ell^2)(|c_+|^2 - |c_-|^2)], \\
d'_3 &= 2\frac{\text{Im}[\vec{n} \cdot (\vec{J} \times \vec{J}^*)]}{|J|^2}[(1 - \hat{m}_\ell^2)(|c_+|^2 - |c_-|^2)] \\
d_4 &= 4\frac{\text{Im}[\vec{n} \cdot (\vec{J} \times \vec{J}^*)]}{|J|^2}(|c_-|^2 + |c_+|^2), \\
d_5 &= -[(1 + \hat{m}_\ell^2)(-|c_-|^2 - |c_+|^2) + 4|c_0|^2 + 4\hat{m}_\ell^2|c_t|^2], \\
d'_5 &= -[(1 - \hat{m}_\ell^2)(4|c_0|^2 - |c_-|^2 - |c_+|^2)].
\end{aligned} \tag{26}$$

Apparently the following combination can be used to extract the hadron amplitude

$$\frac{d_3 + d'_3}{d_2 + d'_2} = \frac{\text{Im}[\vec{n} \cdot (\vec{J} \times \vec{J}^*)]}{|J|^2}. \tag{27}$$

Including the phase-space, we arrive at the angular distribution for $D \rightarrow K_1\ell^+\nu_\ell \rightarrow K\pi\pi\ell^+\nu_\ell$ as:

$$\begin{aligned}
\frac{d\Gamma}{dq^2 d \cos \theta_\ell d \cos \theta_K} &= \frac{G_F^2 |V_{cs}|^2 q^2 \sqrt{\lambda(m_D^2, m_{K_1}^2, q^2)}}{512\pi^3 m_D^3} (1 - \hat{m}_\ell^2)^2 \\
&\times \frac{3}{8} \left(d_1 + d'_1 [\cos^2 \theta_K \cos^2 \theta_\ell] + d_2 \cos \theta_\ell + d'_2 \cos^2 \theta_K \cos \theta_\ell \right. \\
&\left. + d_3 \cos \theta_K + d'_3 \cos \theta_K \cos^2 \theta_\ell + d_4 \cos \theta_K \cos \theta_\ell + d_5 \cos^2 \theta_K + d'_5 \cos^2 \theta_\ell \right).
\end{aligned} \tag{28}$$

The ratio of differential up-down asymmetries proposed in Ref. [23] is evaluated as:

$$\begin{aligned}
\mathcal{A}'_{\text{UD}} &\equiv \frac{\frac{d\Gamma}{dq^2}[\cos \theta_K > 0] - \frac{d\Gamma}{dq^2}[\cos \theta_K < 0]}{\frac{d\Gamma}{dq^2}[\cos \theta_\ell > 0] - \frac{d\Gamma}{dq^2}[\cos \theta_\ell < 0]} \\
&= \frac{3d_3 + d'_3}{3d_2 + d'_2} \\
&= \frac{\text{Im}[\vec{n} \cdot (\vec{J} \times \vec{J}^*)]}{|J|^2} \frac{(2 + \hat{m}_\ell^2)(|c_-|^2 - |c_+|^2)}{2[(|c_-|^2 - |c_+|^2) + 2\text{Re}[c_0c_t^*]\hat{m}_\ell^2]}.
\end{aligned} \tag{29}$$

If the massless limit $\hat{m}_\ell \rightarrow 0$, the above ratio is reduced to the hadronic amplitude $\frac{\text{Im}[\vec{n} \cdot (\vec{J} \times \vec{J}^*)]}{|J|^2}$, but apparently this reduction is contaminated by the lepton mass.

F. Angular Distributions in $B \rightarrow K_1\gamma$

This subsection gives the angular distribution in $B \rightarrow K_1(\rightarrow K\pi\pi)\gamma$. The effective Hamiltonian for $b \rightarrow s\gamma$ has the general form:

$$\begin{aligned}
\mathcal{H}_{\text{eff}} &= -\frac{4G_F}{\sqrt{2}} V_{tb} V_{ts}^* (C_{7L} \mathcal{O}_{7L} + C_{7R} \mathcal{O}_{7R}), \\
\mathcal{O}_{7L,R} &= \frac{em_b}{16\pi^2} \bar{s} \sigma_{\mu\nu} \frac{1 \pm \gamma_5}{2} b F^{\mu\nu},
\end{aligned} \tag{30}$$

TABLE I: The $D \rightarrow K_1$ form factors calculated in the covariant LFQM [26]. The physical K_1 states ($K_1(1270)$ and $K_1(1420)$) are mixtures of the K_{1A} (3P_1) and K_{1B} (1P_1).

F	$F(0)$	a	b	F	$F(0)$	a	b
$A^{DK_{1A}}$	$0.15_{-0.01+0.01}^{+0.01-0.01}$	$0.89_{-0.03+0.00}^{+0.03-0.01}$	$0.12_{-0.02+0.01}^{+0.02-0.01}$	$V_0^{DK_{1A}}$	$0.28_{-0.00+0.00}^{+0.00-0.00}$	$0.84_{-0.02+0.01}^{+0.01-0.01}$	$0.39_{-0.05+0.04}^{+0.06-0.03}$
$V_1^{DK_{1A}}$	$1.60_{-0.05+0.01}^{+0.05-0.02}$	$-0.22_{-0.00+0.03}^{+0.00-0.03}$	$0.07_{-0.00+0.00}^{+0.00-0.00}$	$V_2^{DK_{1A}}$	$0.01_{-0.00+0.00}^{+0.00-0.00}$	$-0.83_{-0.17+0.02}^{+0.15-0.03}$	$0.24_{-0.03+0.01}^{+0.04-0.01}$
$A^{DK_{1B}}$	$0.10_{-0.00+0.00}^{+0.00-0.00}$	$0.98_{-0.01+0.01}^{+0.01-0.01}$	$0.37_{-0.03+0.04}^{+0.03-0.03}$	$V_0^{DK_{1B}}$	$0.48_{-0.01+0.01}^{+0.01-0.03}$	$0.94_{-0.02+0.01}^{+0.01-0.02}$	$0.22_{-0.00+0.03}^{+0.00-0.03}$
$V_1^{DK_{1B}}$	$1.58_{-0.03+0.03}^{+0.02-0.05}$	$0.31_{-0.02+0.02}^{+0.02-0.01}$	$0.04_{-0.00+0.01}^{+0.00-0.00}$	$V_2^{DK_{1B}}$	$-0.13_{-0.01+0.01}^{+0.01-0.01}$	$0.57_{-0.06+0.01}^{+0.04-0.01}$	$0.32_{-0.03+0.06}^{+0.05-0.04}$

where $C_{7L,7R}$ are the corresponding Wilson coefficients for $\mathcal{O}_{7L,R}$, and V_{tb}, V_{ts} are CKM matrix elements. Due to the chirality structure of W^\pm in SM, the photon in $b \rightarrow s\gamma$ is predominantly left-handed, while the right-handed polarization is suppressed by approximately m_s/m_b .

Using the helicity amplitude technique one can similarly calculate the angular distributions for $B \rightarrow K_1(\rightarrow K\pi\pi)\gamma$, and the results are easier in two aspects. First, there is no leptonic part in the decay cascade. Secondly, the $B \rightarrow K_1\gamma$ decay amplitudes only contain two polarizations. Without including higher order QCD corrections, these two polarizations are proportional to $C_{7L,7R}$. So $B \rightarrow K_1(\rightarrow K\pi\pi)\gamma$ has the differential decay rate [17, 18, 22]:

$$\frac{d\Gamma_{K_1\gamma}}{d\cos\theta_K} = \frac{|A|^2|\vec{J}|^2}{4} \times \left[1 + \cos^2\theta_K + 2\lambda_\gamma \cos\theta_K \frac{\text{Im}[\vec{n} \cdot (\vec{J} \times \vec{J}^*)]}{|\vec{J}|^2} \right]. \quad (31)$$

In this equation, the nonperturbative amplitude A characterizes the $B \rightarrow K_1\gamma$, and the θ_K is the same angle as in Fig. 1. The photon helicity λ_γ is

$$\lambda_\gamma \equiv \frac{|\mathcal{A}(B \rightarrow K_{1R}\gamma_R)|^2 - |\mathcal{A}(B \rightarrow K_{1L}\gamma_L)|^2}{|\mathcal{A}(B \rightarrow K_{1R}\gamma_R)|^2 + |\mathcal{A}(B \rightarrow K_{1L}\gamma_L)|^2}, \quad (32)$$

with $\lambda_\gamma \simeq -1$ for $b \rightarrow s\gamma$ but $\lambda_\gamma \simeq +1$ for $\bar{b} \rightarrow \bar{s}\gamma$ in SM.

III. NUMERICAL RESULTS AND DISCUSSIONS

A. K_1 mixing and $D \rightarrow K_1$ form factors

Since strange quark is heavier than up/down quark, $K_1(1270)$ and $K_1(1400)$ are not purely K_{1A} (3P_1) and K_{1B} (1P_1) states, and instead they mix:

$$|K_1(1270)\rangle = |K_{1A}\rangle \sin\Theta_K + |K_{1B}\rangle \cos\Theta_K, \quad (33)$$

$$|K_1(1400)\rangle = |K_{1A}\rangle \cos\Theta_K - |K_{1B}\rangle \sin\Theta_K. \quad (34)$$

The mixing angle Θ_K can be determined by decays such as $\tau^- \rightarrow K_1^- \nu_\tau$, whose decay rate is

$$\Gamma(\tau^- \rightarrow K_1^- \nu_\tau) = \frac{m_\tau^3}{16\pi} G_F^2 |V_{us}|^2 f_A^2 \left(1 - \frac{m_A^2}{m_\tau^2} \right)^2 \left(1 + \frac{2m_A^2}{m_\tau^2} \right). \quad (35)$$

From the measured branching fractions [27]

$$\mathcal{B}(\tau^- \rightarrow K_1(1270)\nu_\tau) = (4.7 \pm 1.1) \times 10^{-3}, \quad (36)$$

$$\mathcal{B}(\tau^- \rightarrow K_1(1400)\nu_\tau) = (1.7 \pm 2.6) \times 10^{-3}, \quad (37)$$

one can determine K_1 decay constants:

$$|f_{K_1(1270)}| = (169_{-21}^{+19})\text{MeV}; \quad |f_{K_1(1400)}| = (125_{-125}^{+74})\text{MeV}. \quad (38)$$

Combing the QCD sum rules for K_{1A} and K_{1B} decay constants [28], one determines the mixing angle with a fourfold ambiguity [24]:

$$-143^\circ < \Theta_K < -120^\circ, \quad \text{or} \quad -49^\circ < \Theta_K < -27^\circ, \quad \text{or} \quad 37^\circ < \Theta_K < 60^\circ, \quad \text{or} \quad 131^\circ < \Theta_K < 153^\circ. \quad (39)$$

TABLE II: Results for integrated branching ratios for the $D \rightarrow K_1(1270)\ell^+\nu_\ell$ and $D \rightarrow K_1(1400)\ell^+\nu_\ell$ decays (in units of 10^{-3}). The experimental results are taken from BESIII measurements [37, 38].

$D^0 \rightarrow K^-(1270)\ell^+\nu_\ell$	\mathcal{B}_L	\mathcal{B}_T	$\mathcal{B}_L/\mathcal{B}_T$	$\mathcal{B}_{\text{total}}$	$\mathcal{B}_{\text{data}}$
$\ell = e$	1.01	0.56	1.80	1.56	$1.09 \pm 0.13^{+0.09}_{-0.13} \pm 0.12$
$\ell = \mu$	0.81	0.49	1.60	1.30	–
$D^+ \rightarrow \bar{K}^0(1270)\ell^+\nu_\ell$	\mathcal{B}_L	\mathcal{B}_T	$\mathcal{B}_L/\mathcal{B}_T$	$\mathcal{B}_{\text{total}}$	$\mathcal{B}_{\text{data}}$
$\ell = e$	2.56	1.41	1.80	3.97	$2.30 \pm 0.26^{+0.18}_{-0.21} \pm 0.25$
$\ell = \mu$	2.06	1.25	1.60	3.31	–
$D^0 \rightarrow K^-(1400)\ell^+\nu_\ell$	\mathcal{B}_L	\mathcal{B}_T	$\mathcal{B}_L/\mathcal{B}_T$	$\mathcal{B}_{\text{total}}$	
$\ell = e$	0.031	0.006	5.60	0.037	–
$\ell = \mu$	0.024	0.005	5.30	0.029	–
$D^+ \rightarrow \bar{K}^0(1400)\ell^+\nu_\ell$	\mathcal{B}_L	\mathcal{B}_T	$\mathcal{B}_L/\mathcal{B}_T$	$\mathcal{B}_{\text{total}}$	
$\ell = e$	0.080	0.014	5.60	0.094	–
$\ell = \mu$	0.062	0.012	5.30	0.074	–

Except the third scenario, the other scenarios are not favored by K_1 masses or $B \rightarrow K_1\gamma$ decay widths [29]. Actually the $\tau \rightarrow K_1\nu$ may give direct information on the K_1 decays [30]. With other available constraints, Ref. [31] suggested the use of $\Theta_K = 50.8^\circ$, while $\Theta_K = 33^\circ$ is suggested in Ref. [32]. In the following we will use $\Theta_K = 60^\circ$ as the central result (which is also favored by BESIII measurements of $\mathcal{B}(D \rightarrow K_1e^+\nu_e)$), but the dependence on Θ_K in a wider range $30^\circ < \Theta_K < 60^\circ$ will be presented.

The $D \rightarrow K_{1A,1B}$ form factors have been calculated in covariant light-front quark model (LFQM) [26, 31–33], and the updated results from Ref. [31] are collected in Tab. I. In the calculation, the q^2 -distribution of form factors is parametrized as:

$$F(q^2) = \frac{F(0)}{1 - aq^2/m_D^2 + b(q^2/m_D^2)^2}, \quad (40)$$

but a different parametrization is adopted for $V_2^{D \rightarrow K_{1B}}$ [26]:

$$F(q^2) = \frac{F(0)}{(1 - q^2/m_D^2)(1 - aq^2/m_D^2 + b(q^2/m_D^2)^2)}. \quad (41)$$

Physical form factors are obtained through:

$$F^{D \rightarrow K_1(1270)} = F^{D \rightarrow K_{1A}} \sin\Theta_K + F^{D \rightarrow K_{1B}} \cos\Theta_K, \quad (42)$$

$$F^{D \rightarrow K_1(1400)} = F^{D \rightarrow K_{1A}} \cos\Theta_K - F^{D \rightarrow K_{1B}} \sin\Theta_K. \quad (43)$$

The $D \rightarrow K_1$ form factors have also been calculated in other approaches [34–36] but results differ significantly.

B. Decay widths and branching fractions

To calculate decay widths, we use the following inputs from Particle Data Group [27]:

$$\begin{aligned} \tau(D^0) &= (0.4101 \pm 0.0015) \times 10^{-12} \text{s}, & \tau(D^+) &= (1.040 \pm 0.007) \times 10^{-12} \text{s}, \\ m_{K_1(1270)} &= 1.253 \text{GeV}, & m_{K_1(1400)} &= 1.403 \text{GeV}, & V_{cs} &= 0.973. \end{aligned} \quad (44)$$

Differential decay widths $d\Gamma/dq^2$ (in units of 10^{-15}GeV^{-1}) for $D \rightarrow K_1(1270)\ell^+\nu_\ell$ and $D \rightarrow K_1(1400)\ell^+\nu_\ell$ are shown in Fig. 2. The dotted and dashed lines correspond to the longitudinal and transverse polarizations, while the solid line gives the total differential decay widths. At low q^2 , the longitudinal polarization dominates.

Results for integrated branching ratios for the $D \rightarrow K_1(1270)\ell^+\nu_\ell$ and $D \rightarrow K_1(1400)\ell^+\nu_\ell$ decays (in units of 10^{-3}) are given in Tab. II. The experimental results are taken from BESIII measurements [37, 38]. Through this table, one can see that the theoretical results for branching fractions of $D \rightarrow K_1(1270)e^+\nu_e$ are larger than the experimental

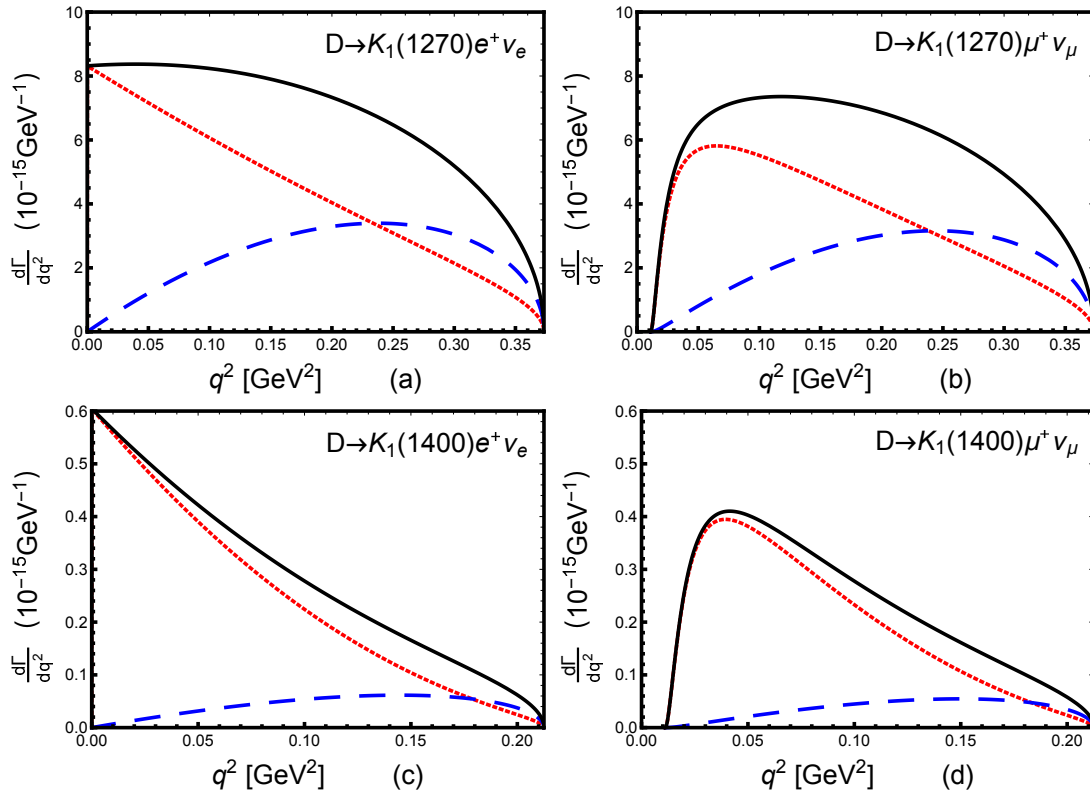


FIG. 2: Differential decay widths for $D \rightarrow K_1(1270)\ell^+\nu_\ell$ (in units of 10^{-15}GeV^{-1}) and $D \rightarrow K_1(1400)\ell^+\nu_\ell$ (in units of 10^{-15}GeV^{-1}). The dotted and dashed lines correspond to the longitudinal and transverse polarizations, while the solid line gives the total differential decay widths.

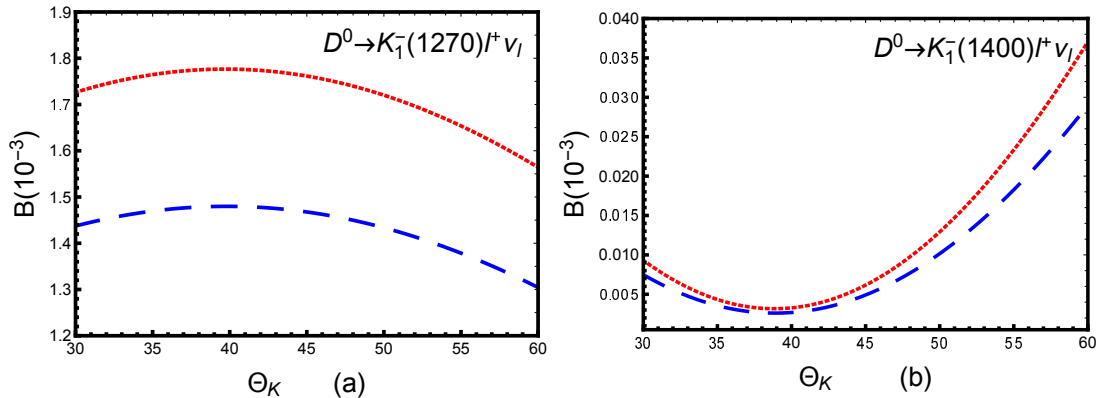


FIG. 3: Dependence of branching ratios $\mathcal{B}(D^0 \rightarrow K_1^-\ell^+\nu_\ell)$ (in units of 10^{-3}) on the mixing angle Θ_K in the range $30^\circ < \Theta_K < 60^\circ$. Dotted and dashed curves correspond to the electron and muon mode, respectively.

data by about a factor of 1.5. However we find that using form factors from Refs. [34–36] the branching fractions can be significantly reduced. Branching fractions for $D \rightarrow K_1(1400)\ell^+\nu_\ell$ are suppressed by orders of magnitudes, and this pattern is consistent with the BESIII observations [37, 38].

Fig. 3 shows the dependence of branching fractions $\mathcal{B}(D^0 \rightarrow K_1^-\ell^+\nu_\ell)$ (in units of 10^{-3}) on the mixing angle Θ_K in the range $30^\circ < \Theta_K < 60^\circ$. Dotted and dashed curves correspond to the electron and muon mode, respectively. Due to the phase space suppression, decays with muon in the final state are typically smaller than the electron mode by approximately 10% – 20%.

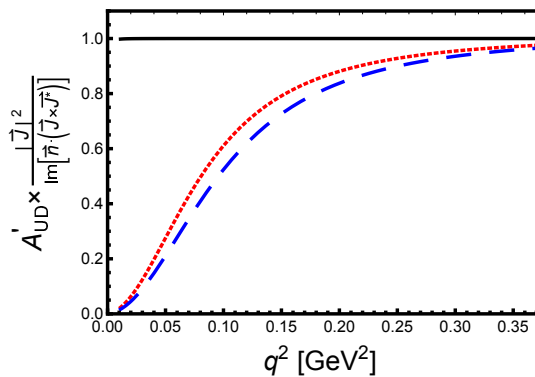


FIG. 4: Results for up-down asymmetry A'_{UD} (in unit of $\text{Im}[\vec{n} \cdot (\vec{J} \times \vec{J}^*)]/|\vec{J}|^2$) in $D \rightarrow K_1(\rightarrow K\pi\pi)\ell^+\nu_\ell$. The solid curve corresponds to the electron final state, in which the lepton mass is negligible and the result is very close to unity. The dashed and dotted results correspond to the muon mode with the mixing angle $\Theta_K = 60^\circ$ and $\Theta_K = 30^\circ$, respectively. The nonzero mass of μ provides sizable corrections as shown in Eq. (29).

C. Angular distributions

Results for up-down asymmetry A'_{UD} (in unit of $\text{Im}[\vec{n} \cdot (\vec{J} \times \vec{J}^*)]/|\vec{J}|^2$) in $D \rightarrow K_1(1270)\ell^+\nu_\ell$ are shown in Fig. 4. The solid curve corresponds to the electron final state, in which the lepton mass is negligible and the result is very close to unity. The dashed and dotted results correspond to the muon mode with the mixing angle $\Theta_K = 60^\circ$ and $\Theta_K = 30^\circ$, respectively. From this figure, one can see that the nonzero mass of muon can give considerable corrections also shown in Eq. (29), but the results are less sensitive to the $D \rightarrow K_1$ form factors.

Integrating over the q^2 , we obtain the angular distributions of $D \rightarrow K_1(\rightarrow K\pi\pi)\ell^+\nu_\ell$ dataset as

$$\frac{d\Gamma}{d\cos\theta_\ell d\cos\theta_K} = a_1 + a_2[\cos^2\theta_K \cos^2\theta_\ell] + a_3 \cos\theta_\ell + a_4 \cos^2\theta_K \cos\theta_\ell + a_5 \cos\theta_K + a_6 \cos\theta_K \cos^2\theta_\ell + a_7 \cos\theta_K \cos\theta_\ell + a_8 \cos^2\theta_K + a_9 \cos^2\theta_\ell, \quad (45)$$

with

$$a_i = \frac{3}{8} \int dq^2 \frac{G_F^2 V_{cs}^2 q^2 \sqrt{\lambda(m_D^2, m_{K_1}^2, q^2)}}{512\pi^3 m_D^3} (1 - m_\ell^2/q^2)^2 \times d_i. \quad (46)$$

As an illustration, we use a standalone fast simulation software RapidSim [39] with the LHCb geometrical acceptance to generate MC samples. $D^0 \rightarrow K_1(1270)^-\mu^+\nu_\mu$ decays are described by EVTGEN [40] with the ISGW2 model [41]. In the simulation, we have generated about 1.7×10^6 events with three decay modes for $K_1(1270)^-$: about 10^6 events for $D \rightarrow K_1(\rightarrow \rho(\rightarrow \pi\pi)K)\mu^+\nu_\mu$, 0.5×10^6 events for $D \rightarrow K_1(\rightarrow K^*(892)(\rightarrow K\pi)\pi)\mu^+\nu_\mu$ and 0.2×10^6 for $D \rightarrow K_1(\rightarrow K\pi\pi)\mu^+\nu_\mu$ in which the K_1 decay is produced according to phase space. A comparison of fitting these MC samples using the formula 45 and the one from previous work [23] is given in Fig. 5, and a detailed analysis of each component is given in Fig. 6. Through these figures, one can see that our simulated angular distributions can not be well described by the angular distribution in the previous work [23]. With the inclusion of the muon mass, the agreement between theoretical description and angular distributions of MC events is greatly improved.

IV. SUMMARY

Weak decays of heavy quarks have played an important role in testing standard model and probing new physics beyond. Recent studies of flavor-changing neutral current process has revealed some hints for potential NP effects (see for instance Ref. [42]), but a conclusive result is far from well-established, and requests more dedicated theoretical and experimental studies in future [43]. At the same time, the photon helicity in $b \rightarrow s\gamma$ might render very competitive potentials for new physics [15].

Based on a previous proposal to pin down hadronic uncertainties in $B \rightarrow K_1\gamma$ [23], we have in this work systematically derived differential decay widths and angular distributions for the decay cascade $D \rightarrow K_1(1270, 1400)\ell^+\nu_\ell \rightarrow (K\pi\pi)\ell^+\nu_\ell$ ($\ell = e, \mu$). In the derivation, the mass of electron/muon is explicitly included. Using the $D \rightarrow K_1$ form factors from light-front quark model, we have calculated partial decay widths and branching fractions for $D^0 \rightarrow K_1^-\ell^+\nu_\ell$

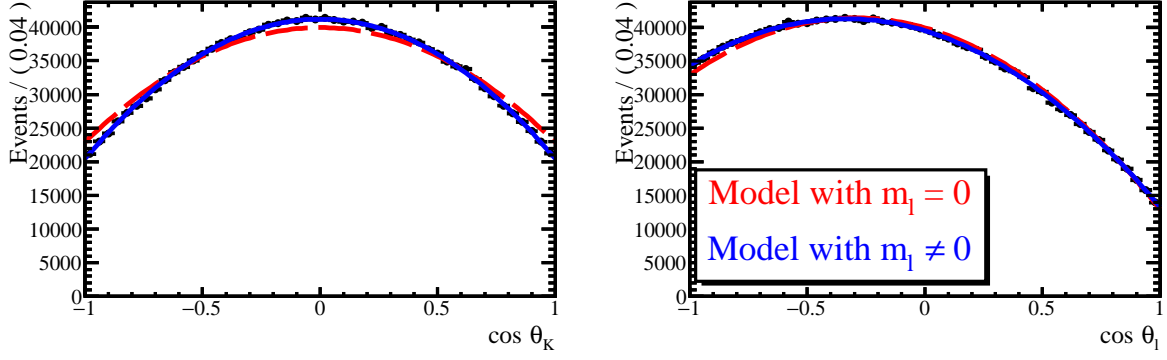


FIG. 5: Fit to 1.7×10^6 MC events with 3 components using two models: $m_l=0$ (Red) and $m_l \neq 0$ (Blue)

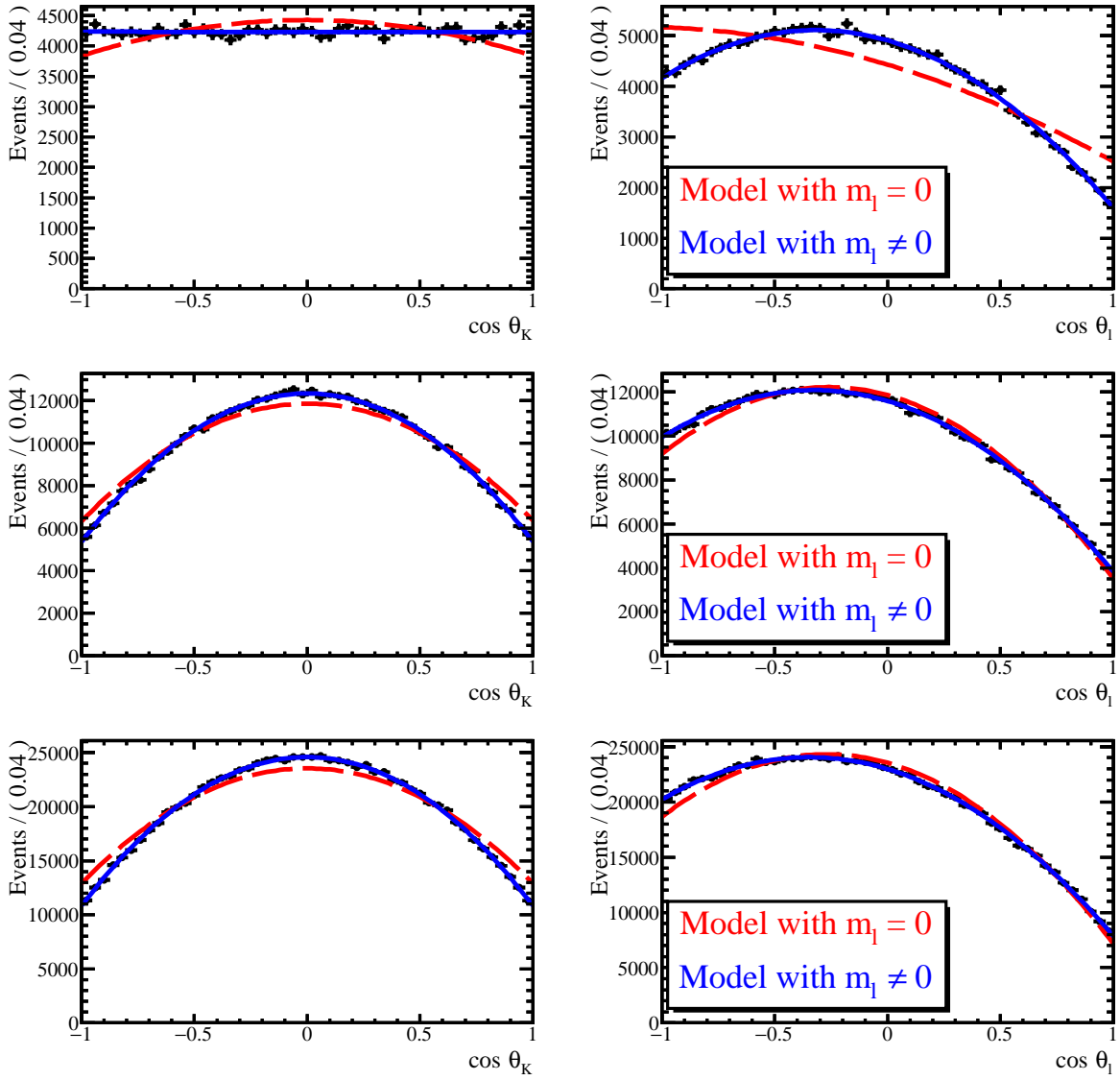


FIG. 6: Fit to 0.2×10^6 $D \rightarrow K_1(\rightarrow K\pi\pi)\mu^+\nu_\mu$ (upper), 0.5×10^6 $D \rightarrow K_1(\rightarrow K^*(892)(\rightarrow K\pi)\pi)\mu^+\nu_\mu$ (middle) and 10^6 $D \rightarrow K_1(\rightarrow \rho(\rightarrow \pi\pi)K)\mu^+\nu_\mu$ (lower) MC events using two models: $m_l=0$ (Red) and $m_l \neq 0$ (Blue)

and $D^+ \rightarrow K_1^0 \ell^+ \nu_\ell$, but pointed out that these theoretical results for $\mathcal{B}(D \rightarrow K_1 e^+ \nu_e)$ are about a factor 1.5 higher than recent BESIII measurements.

With the angular coefficients, we have demonstrated that the measurement of up-down asymmetry in $D \rightarrow K_1 e^+ \nu_e \rightarrow (K\pi\pi)e^+ \nu_e$ and the angular distribution in $D \rightarrow K_1 \ell^+ \nu_\ell \rightarrow (K\pi\pi)\ell^+ \nu_\ell$ can help to pin down hadronic uncertainties in $B \rightarrow K_1(\rightarrow K\pi\pi)\gamma$. Based on the Monte-Carlo simulation, we have found that after including the muon mass, the angular distributions can be well described by the theoretical framework.

Acknowledgement

W.W. thanks Fu-Sheng Yu and Zhen-Xing Zhao for valuable discussions and the collaboration at the early stage of this work. The authors are grateful to Fei Huang, Xian-Wei Kang, Xiao-Rui Lyu, Wen-Bin Qian, Yang-Heng Zheng for useful discussions. This work is supported in part by Natural Science Foundation of China under grant No.11735010, U1932108, U2032102, 12061131006, and 12061141006, by Natural Science Foundation of Shanghai under grant No. 15DZ2272100.

-
- [1] D. Atwood, M. Gronau and A. Soni, Phys. Rev. Lett. **79**, 185-188 (1997) doi:10.1103/PhysRevLett.79.185 [arXiv:hep-ph/9704272 [hep-ph]].
 - [2] D. Becirevic, E. Kou, A. Le Yaouanc and A. Tayduganov, JHEP **08**, 090 (2012) doi:10.1007/JHEP08(2012)090 [arXiv:1206.1502 [hep-ph]].
 - [3] A. Paul and D. M. Straub, JHEP **04**, 027 (2017) doi:10.1007/JHEP04(2017)027 [arXiv:1608.02556 [hep-ph]].
 - [4] E. Kou, C. D. Lü and F. S. Yu, JHEP **12**, 102 (2013) doi:10.1007/JHEP12(2013)102 [arXiv:1305.3173 [hep-ph]].
 - [5] N. Haba, H. Ishida, T. Nakaya, Y. Shimizu and R. Takahashi, JHEP **03**, 160 (2015) doi:10.1007/JHEP03(2015)160 [arXiv:1501.00668 [hep-ph]].
 - [6] B. Aubert *et al.* [BaBar], Phys. Rev. D **77**, 051103 (2008) doi:10.1103/PhysRevD.77.051103 [arXiv:0711.4889 [hep-ex]].
 - [7] J. P. Lees *et al.* [BaBar], Phys. Rev. Lett. **109**, 191801 (2012) doi:10.1103/PhysRevLett.109.191801 [arXiv:1207.2690 [hep-ex]].
 - [8] J. P. Lees *et al.* [BaBar], Phys. Rev. D **86**, 052012 (2012) doi:10.1103/PhysRevD.86.052012 [arXiv:1207.2520 [hep-ex]].
 - [9] T. Saito *et al.* [Belle], Phys. Rev. D **91**, no.5, 052004 (2015) doi:10.1103/PhysRevD.91.052004 [arXiv:1411.7198 [hep-ex]].
 - [10] Y. Ushiroda *et al.* [Belle], Phys. Rev. D **74**, 111104 (2006) doi:10.1103/PhysRevD.74.111104 [arXiv:hep-ex/0608017 [hep-ex]].
 - [11] B. Aubert *et al.* [BaBar], Phys. Rev. D **78**, 071102 (2008) doi:10.1103/PhysRevD.78.071102 [arXiv:0807.3103 [hep-ex]].
 - [12] R. Aaij *et al.* [LHCb], Phys. Rev. Lett. **123**, no.8, 081802 (2019) doi:10.1103/PhysRevLett.123.081802 [arXiv:1905.06284 [hep-ex]].
 - [13] S. Akar, E. Ben-Haim, J. Hebing, E. Kou and F. S. Yu, JHEP **09**, 034 (2019) doi:10.1007/JHEP09(2019)034 [arXiv:1802.09433 [hep-ph]].
 - [14] Y. Grossman and D. Pirjol, JHEP **06**, 029 (2000) doi:10.1088/1126-6708/2000/06/029 [arXiv:hep-ph/0005069 [hep-ph]].
 - [15] R. Aaij *et al.* [LHCb], JHEP **12**, 081 (2020) doi:10.1007/JHEP12(2020)081 [arXiv:2010.06011 [hep-ex]].
 - [16] S. de Boer and G. Hiller, Eur. Phys. J. C **78**, no.3, 188 (2018) doi:10.1140/epjc/s10052-018-5682-7 [arXiv:1802.02769 [hep-ph]].
 - [17] M. Gronau, Y. Grossman, D. Pirjol and A. Ryd, Phys. Rev. Lett. **88**, 051802 (2002) doi:10.1103/PhysRevLett.88.051802 [arXiv:hep-ph/0107254 [hep-ph]].
 - [18] M. Gronau and D. Pirjol, Phys. Rev. D **66**, 054008 (2002) doi:10.1103/PhysRevD.66.054008 [arXiv:hep-ph/0205065 [hep-ph]].
 - [19] E. Kou, A. Le Yaouanc and A. Tayduganov, Phys. Rev. D **83**, 094007 (2011) doi:10.1103/PhysRevD.83.094007 [arXiv:1011.6593 [hep-ph]].
 - [20] R. Aaij *et al.* [LHCb], Phys. Rev. Lett. **112**, no.16, 161801 (2014) doi:10.1103/PhysRevLett.112.161801 [arXiv:1402.6852 [hep-ex]].
 - [21] A. Tayduganov, E. Kou and A. Le Yaouanc, Phys. Rev. D **85**, 074011 (2012) doi:10.1103/PhysRevD.85.074011 [arXiv:1111.6307 [hep-ph]].
 - [22] M. Gronau and D. Pirjol, Phys. Rev. D **96**, no.1, 013002 (2017) doi:10.1103/PhysRevD.96.013002 [arXiv:1704.05280 [hep-ph]].
 - [23] W. Wang, F. S. Yu and Z. X. Zhao, Phys. Rev. Lett. **125**, no.5, 051802 (2020) doi:10.1103/PhysRevLett.125.051802 [arXiv:1909.13083 [hep-ph]].
 - [24] R. H. Li, C. D. Lu and W. Wang, Phys. Rev. D **79**, 034014 (2009) doi:10.1103/PhysRevD.79.034014 [arXiv:0901.0307 [hep-ph]].
 - [25] W. Wang and Z. X. Zhao, Eur. Phys. J. C **76**, no.2, 59 (2016) doi:10.1140/epjc/s10052-016-3900-8 [arXiv:1511.06998 [hep-ph]].

- [26] H. Y. Cheng, C. K. Chua and C. W. Hwang, Phys. Rev. D **69**, 074025 (2004) doi:10.1103/PhysRevD.69.074025 [arXiv:hep-ph/0310359 [hep-ph]].
- [27] P. A. Zyla *et al.* [Particle Data Group], PTEP **2020**, no.8, 083C01 (2020) doi:10.1093/ptep/ptaa104
- [28] K. C. Yang, Nucl. Phys. B **776**, 187-257 (2007) doi:10.1016/j.nuclphysb.2007.03.046 [arXiv:0705.0692 [hep-ph]].
- [29] K. Abe *et al.* [Belle], [arXiv:hep-ex/0408138 [hep-ex]].
- [30] K. Hayasaka, Z. Huang and E. Kou, [arXiv:2102.00752 [hep-ph]].
- [31] R. C. Verma, J. Phys. G **39**, 025005 (2012) doi:10.1088/0954-3899/39/2/025005 [arXiv:1103.2973 [hep-ph]].
- [32] H. Y. Cheng and X. W. Kang, Eur. Phys. J. C **77**, no.9, 587 (2017) [erratum: Eur. Phys. J. C **77**, no.12, 863 (2017)] doi:10.1140/epjc/s10052-017-5170-5 [arXiv:1707.02851 [hep-ph]].
- [33] Q. Chang, X. L. Wang and L. T. Wang, Chin. Phys. C **44**, no.8, 083105 (2020) doi:10.1088/1674-1137/44/8/083105 [arXiv:2003.10833 [hep-ph]].
- [34] S. Momeni and R. Khosravi, J. Phys. G **46**, no.10, 105006 (2019) doi:10.1088/1361-6471/ab35d0 [arXiv:1903.00860 [hep-ph]].
- [35] R. Khosravi, K. Azizi and N. Ghahramany, Phys. Rev. D **79**, 036004 (2009) doi:10.1103/PhysRevD.79.036004 [arXiv:0812.1352 [hep-ph]].
- [36] S. Momeni, Eur. Phys. J. C **80**, no.6, 553 (2020) doi:10.1140/epjc/s10052-020-8084-6 [arXiv:2004.02522 [hep-ph]].
- [37] M. Ablikim *et al.* [BESIII], Phys. Rev. Lett. **123**, no.23, 231801 (2019) doi:10.1103/PhysRevLett.123.231801 [arXiv:1907.11370 [hep-ex]].
- [38] M. Ablikim *et al.* [BESIII], [arXiv:2102.10850 [hep-ex]].
- [39] G. A. Cowan, D. C. Craik and M. D. Needham, Comput. Phys. Commun. **214**, 239-246 (2017) doi:10.1016/j.cpc.2017.01.029 [arXiv:1612.07489 [hep-ex]].
- [40] D. J. Lange, Nucl. Instrum. Meth. A **462**, 152-155 (2001) doi:10.1016/S0168-9002(01)00089-4
- [41] D. Scora and N. Isgur, Phys. Rev. D **52**, 2783-2812 (1995) doi:10.1103/PhysRevD.52.2783 [arXiv:hep-ph/9503486 [hep-ph]].
- [42] R. Aaij *et al.* [LHCb], [arXiv:2103.11769 [hep-ex]].
- [43] A. Cerri, V. V. Gligorov, S. Malvezzi, J. Martin Camalich, J. Zupan, S. Akar, J. Alimena, B. C. Allanach, W. Altmannshofer and L. Anderlini, *et al.* CERN Yellow Rep. Monogr. **7**, 867-1158 (2019) doi:10.23731/CYRM-2019-007.867 [arXiv:1812.07638 [hep-ph]].